Est. 1984

ORIENTAL JOURNAL OF CHEMISTRY
An International Open Free Access, Peer Reviewed Research Journal

www.orientjchem.org

ISSN: 0970-020 X
CODEN: OJCHEG
2014, Vol. 30, No. (4):
Pg. 1577-1584

Preparation of TiO_2/SiO_2 Nanocomposite with Non-ionic Surfactants via Sol-gel Process and their Photocatalytic Study

RUCHI NANDANWAR[1], PURNIMA SINGH[1], FAZIL F. SYED[2] and FOZIA Z. HAQUE[3]*

[1]Department of Physics, Sarojini Naidu Govt. Girls P.G. (Autonomous) College, Barkatullah University, Bhopal - 462016, India
[2] Department of Chemistry, Mumbai University, Mumbai - 400 032, Maharashtra, India
[3]Department of Physics, Maulana Azad National Institute of Technology, Bhopal, India,
*Corresponding author E-mail: foziazia@rediffmail.com

http://dx.doi.org/10.13005/ojc/300417

(Received: July 25, 2014; Accepted: September 01, 2014)

ABSTRACT

TiO_2/SiO_2 nanocomposite particles were prepared from TTIP precursor for titania and TEOS precursor for silica, by using a sol-gel method at low temperature in acidic pH with various templates: poly(ethylene glycol) (PEG) and Triton X-100 (TX-100). The properties of resulting Ti/Si nanocomposites materials were characterized by X-ray diffraction (XRD), Scanning Electron Microscopy (SEM), UV-Vis absorption spectroscopy; Photo-Luminescence spectra and Fourier transform infrared (FTIR) techniques. The results show that the TS cores were uniformly coated by Triton X-100 having spherical nanoparticles. XRD result showed that $TS:T_X$ smaller crystallite size than the $TS:T_X$ nanocomposite particles and both samples include anatase phase. The UV–Vis spectrum of as-synthesized samples shows absorption in the visible range. The PL emission intensity of $TS:T_X$ nanocomposite was slightly decreased compared with $TS:P_{EG}$ nanocomposite due to decrease in recombination rate. From FTIR results metal oxide stretching was confirmed in both the samples. The photocatalytic activity of samples was tested for degradation of methylene blue (MB) solutions. The results clearly showed that Triton X-100 coated TS sample exhibited higher activity than that of $TS:P_{EG}$ under UV irradiation, due to the low recombination rate of photo-generated electrons and holes.

Key words: TiO_2/SiO_2, nanocomposite, sol-gel method, non-ionic surfactants, morphology, optical properties, XRD, FT-IR.

INTRODUCTION

Titanium dioxide nanomaterials have been intensively studied because of their unique properties, various uses[1,2] and versatile applications, for example, in photocatalysis, optoelectronic devices, environmental purification, photo-eletrochemical solar energy conversion and optical coating[3,4]. There are several techniques for synthesizing titania nanoparticles through

controlled nucleation and growth processes in dilute Ti (IV) solutions[5-7]. Among them the sol-gel process is one of the most convenient ways to synthesize various metal oxides due to some advantages, such as homogeneity at molecular level, a wide range of a precursor selection, control over microstructure, low demands upon reagent purity, possibility of a fine adjustment of the end product properties and low processing temperature[8].

TiO_2 crystallizes in three types: anatase, rutile and brookite. Among the three, crystalline titania, especially its anatase phase is an n-type semiconductor[9, 10] has most stable modification[11]. Most researchers have paid greater attention to TiO_2 anatase phase in photocatalytic reactions and photo-electrochemical cell its potential application in degradation of various environmental pollutants under ultraviolet (UV) irradiation[12] in both gaseous and liquid phases because of its strong oxidizing power, non-toxicity and long-term photo-stability[13, 14]. For more than a decade, studies have mainly concentrated on the suspension of TiO_2 fine powder because of its higher photocatalytic activity photo-degrade pollutant molecules when radiated with UV radiation compared to TiO_2 thin films[15]. TiO_2 powders possess interesting optical, dielectrical, and catalytical properties, which results in industrial applications[16, 18]. In recent years great efforts have been devoted to the study of TiO_2 materials for photocatalytic degradation of organic and inorganic contaminants of water and air[19-20]. The synthesis of TiO_2 by the sol-gel method has proven to be a very useful tool for photo-induced molecular reactions to take place on a titanium dioxide surface[21]. Titania has band gap energy of around 3.2 eV and is therefore a UV absorber. When TiO_2 is subjected to UV light (λ > 385 nm), an electron/hole pair (e_{CB}^-/ h_{VB}^+) is generated. Photo-catalytic reactions take place primarily on the surface of TiO_2, where the photo-generated electrons and holes are trapped. In general, good crystalline materials with optimum surface area are ideal candidates as photocatalysts.

Recently, titania-silica composite materials have been obtained by sol–gel method due to its possible capability in controlling the textural and surface properties of the composite, to offer unique advantages for the preparation of such highly dispersed tetrahedrally coordinated and transparent photocatalysts material[22]. This sol-gel process provides to synthesis mesoporous TiO_2/ SiO_2 composite materials to enhanced stability, textural properties and surface area useful for applications as catalysts and solar-cells[23, 24]. SiO_2 has high thermal stability, good carriers properties and excellent mechanical strength widely used in organics compounds to active sites on TiO_2 particles[24-27]. The addition of SiO_2 on TiO_2 matrix suppresses the crystal growth of TiO_2 and enhanced the photocatalytic performance[28]. Abdolreza Nilchi[29] et.al reported that the sol-gel produced TiO_2/SiO_2 nanocomposite has good photocatalytic properties due to its anatase phase, existence of tetrahedral coordination of TiO_2 in the SiO_2 matrix and very large surface area. Kim et.al, [30] proposed two models for titanium dioxide activation in the presence of silicon dioxide. There are two types of interaction between TiO_2 and SiO_2: physically mixed and chemically bonded[31]. Shaozheng Hu et.al studied the SiO_2-coated TiO_2 composite materials with enhanced photocatalytic activity under UV light was prepared by a simple catalytic hydrolysis method[32].

There is a growing interest in the development of nanocomposites consisting of organic polymers and titania or amorphous silica nanoparticles. Mosurkal et.al view nanocomposites of siloxane copolymers and nano-TiO_2 as 'environmentally safe' [33]. The textural properties of TiO_2-SiO_2 composites synthesized by sol-gel process were successively enhanced using surfactant to enhance the photocatalytic properties[34]. The TiO_2-SiO_2 coatings were also prepared with poly-ethylene-glycol (PEG) to lower the sol-gel processing temperature to examine bio-compatibility of new biomaterials and derived implant coatings[35]. The formation of nanocomposites by the sol–gel method has been reported to be strongly dependent on the choice of a solvent and a foreign stabilizing surfactant. To synthesize TiO_2-SiO_2 nanocomposites at room temperature with the addition of polymer (PVA) could effectively suppress the particle growth and improve the stability of TS hydrosols[36]. Kimura Isao *et.al* reported the preparation of composite microspheres suspended in dye solution under ultraviolet irradiation and examined the possibility of applying to wastewater treatment[37].

In this work, a novel sol–gel method was employed for the synthesis of TiO_2-SiO_2 nanocomposite particles with non-ionic surfactants polyethylene glycol (PEG) and polyethylene glycol tert-octylphenyl ether (Triton X-100) at low temperature. Photocatalytic degradation activities of the synthesized particles were studied using Methylene Blue (MB) as a model organic compound under UV light irradiation.

EXPERIMENTAL

Materials

In this synthesis procedure, we use tetraethoxysilane (TEOS) (99.9 %, Sigma Aldrich) as a precursor material of SiO_2 and titanium tetra-isopropoxide (TTIP) (99.9 %, Sigma Aldrich) as a precursor material of TiO_2. Concentrated hydrochloric-acid (HCl) (99.9 %, Merck) as a catalyst and solvents absolute ethanol (99.9 %, Merck), polyethylene glycol (PEG) (M_w= 570 gram/mole), and polyethylene glycol tert-octylphenyl ether (Triton X-100) (M_w= 646.87 gram/mole) (99.9 %, Merck) were used without any further purification. Methylene Blue (MB) (Sigma Aldrich) was used a model organic compound for Photocatalytic study. Deionised water was used throughout the experiments. The synthesis was carried out in the continuous stirring at the temperature of 60°C. The stirring was conducted using an electromagnetic stirrer with a stirring speed of ca. 1100 rpm.

Synthesis of titania/silica with surfactants composite

In the synthesis of TiO_2/SiO_2 composite particles were prepared according. Titanium tetra-isopropoxide (TTIP) (1 mole) prepared by dissolving in solvent ethanol (10 ml), and deionized water (35 ml) mixture was stirred for 10 min, pH range of 2.5. And, then added, catalyst hydrochloric-acid (HCl) (1 mole) drop-wise into the above mixture and magnetically stirred for 30 min. at temperature 60°C, in the pH range 1, to become a yellowish homogeneous transparent solution. Then, 1 mole of silica precursor material tetraethoxysilane (TEOS) was slowly added in the titania sol phase and the mixture was stirred for 1 hour at 60 °C. The surfactant (0.1 mole) was added to the above mixture was stirred for 1 hour at temperature 60°C. A white lump free paste was formed. The resulting pastes were dried at room temperature during 1 month. Finally, the product was grinded into a powder to obtain fine white powder and used for further material characterization. For convenience, the abbreviations TiO_2/SiO_2 prepared with surfactant PEG is denoted as TS:P_{EG} and with surfactant Triton X-100 is denoted as TS:T_X respectively.

Characterization

The prepared titania-silica composite nanoparticles were characterized for surface morphology was studied using scanning electron microscopy (SEM) (Model JEOL- JSM- 6390). Powder X-ray diffraction measurement was carried out using Bruker D8 Advance X-ray diffract-metre. The X-rays were produced using a sealed tube and the wavelength X-ray was 0.154 nm (CuK-alpha). The X-rays were detected using a fast counting detector based on Silicon strip technology (Bruker LynxEye detector). The optical properties studied using UV–Visible absorption spectra were recorded with a Carry 5000 UV-Vis-NIR spectrometer, and emission spectra were observed by photoluminescence spectroscopy (F-7000, Hitachi spectrophotometer) with excitation wavelength (λ_{ex}) = 350nm using xenon lamp as source at room temperature.. The FTIR spectra were measured on a Bruker Model-Vertex 70-Spectroscopy with a wave number range of 1000 to 4000 cm^{-1}.

Measurement of photocatalytic activity

The photocatalytic performances of the synthesized composite particles were studied by the degradation experiments using Methylene Blue (MB) dye as a model compound under ultraviolet light irradiation. An UV Xenon lamp with 125 W was used as UV source. Photocatalysis experiments were performed in a self designed photo-oxidation reactor which is a dark black box. The test materials was kept in a glass beaker covered with aluminum foil to prevent light from other sources from entering the beaker. This ensured that all light came from one direct source. The lamp was fitted on the top of the reactor. The distance between lamp and photocatalysis system was about 1 cm. Prior to illumination, a suspension containing 0.05g of powder catalyst was added 1 ml L^{-1} MB (10^{-4}) aqueous solution was mixed in a glass beaker and magnetically stirred in dark for

30 min., to attain adsorption equilibrium and the solution was exposed to UV-visible irradiation. The experiment was performed at room temperature. At regular intervals, 5 ml solution were taken from the reactor and centrifuged to remove the photocatalyst before analysis by UV-visible spectrometer at 664 nm corresponding to maximum absorption wavelength (λ_{max}) of MB.

RESULTS AND DISCUSSION

SEM characterization

The study of morphologies of the powder samples of Ti/Si nano composite with surfactants PEG and Tritonx-100 was observed with SEM as shown in Fig. 1 (a) (b).

As it can be seen in Fig. 1 (a), the TS:P_{EG} nanocomposite consists of irregular morphology due to the agglomeration of primary particles, which may cause the surface to be non-uniform and ill-defined. In Fig. 1 (b), the accumulation of particle indicates packed and dense structure. Whereas TS:T_X nanocomposite particles exhibited regular morphology since the TS cores were uniformly coated by Triton X-100 and having well-structured granular nano-surface with clear interstices between the particles/aggregates. The TS:T_X nanocomposite powder particles show the formation of uniform spherical and narrowly dispersed particles.

X-ray diffraction analysis

The XRD diffraction patterns of sol–gel-derived nano TS:P_{EG} and TS:T_X composites were carried out on powder form are shown in Fig. 2. The crystallite type of the TS nanocomposite particles was the pure anatase. In the diffraction pattern, it is clearly assigned that the peaks of SiO_2 are not observed because they are mainly amorphous in nature, and the diffractogram consist strongest diffraction peaks of TiO_2 in anatase phase (with the reference pattern (JCPDS 21-1272) of TiO_2).

The powder samples showed the crystalline pattern and the observed d_{101} lines match the reported values for the anatase phase. The average crystallite size of the samples was determined from Scherrer's equation[38] using the (101) reflections of the anatase phase assuming spherical particles. Using the Scherrer's formula, D

Table 1: Crystallite size, 2¸ angle (degree), unit cell volume and optical band gap of the as-synthesized samples

Sample	θ(degree)	Crystallite size (nm)	Unit cell volume (A^{o3})	Optical band gap E_g (eV)
TS-PEG	25.181	3.51	134.72	3.5221
TS-Triton X-100	25.484	3.49	136.30	3.0995

= K λ/ ² cos¸, an estimate of the grain size (D) from the broadening of the main (101) anatase peak can be done, K is a constant depend on the crystallite shape (0.9), λ is the X-ray wavelength (in this case, λ = 1.5418 Å for Cu-K_α radiation), β is the full width at half maxima (FWHM) of the diffraction peaks (radian) and ¸ is the Bragg's angle and also the unit cell volume as correlated to reference pattern as shown in Table 1.

The observed d_{101} anatase line for TS:T_X sample is very broader and weaker than the TS:P_{EG} sample. The broadening of the XRD peaks indicates that the particles are of very small crystallite size in nature[39]. The introduction of SiO_2 can reduce the growth rate of anatase titania nanoparticle. The TS:T_X nanoparticles growth is retarded due to the Si atom with Triton X-100, this agree with the small value of grain size and effectively increase the stability of anatase TiO_2. The result illustrates that Triton X-100 template induces the formation of small and uniform anatase crystallite sizes. The diffraction peak intensity of the TS:T_X composite material shows the high crystallinity than nano TS:P_{EG} composite nanoparticle, resulting in production of more charge carriers and high surface area for photocatalytic activity. It is obviously shown that the TS:T_X prepared powder sample is completely crystalline than TS:P_{EG} and entirely consists of anatase phase.

UV-visible absorption spectra

The UV–Visible absorption spectra of as-synthesized samples show in Fig. 3. It can be seen that the TS:P_{EG} nanocomposites exhibited an absorption edge at 352 nm in Fig. 3a. The absorption edge of TS:T_X nanocomposite slightly falls into the visible region at the wavelength of 400 nm as shown in Fig. 3b. The optical band gap can be calculated by the equation: E_g =1239.8/ » where E_g is the band gap (eV) and λ (nm) is the wavelength of the absorption edge in the spectrum. The optical band gaps E_g for both the synthesized samples were estimated and tabulated in Table 1.

Both the as-synthesized samples show slightly similar absorption pattern, in which the TS:T_X nanocomposite shows better absorbance in visible range compared to TS:P_{EG} nano composite particles. Furthermore, due to the higher dispersity and the coverage of SiO_2 on TiO_2 surface restrained the absorption of UV light irradiation. In addition, the absorption spectra of the TS:T_X sample shows stronger absorbance than TS:P_{EG} nanocomposite particle under UV irradiation, indicating that TS:T_X could be a promising approach for increasing the catalytic activity.

PL spectroscopy analysis

A photo luminescence spectrum in emission mode is done in the full spectrum range from 200 nm to 700 nm. Fig. 4 shows the PL emission spectrum of TS:P_{EG} and TS:T_X nanocomposite samples at the excitation wavelength of 350 nm.

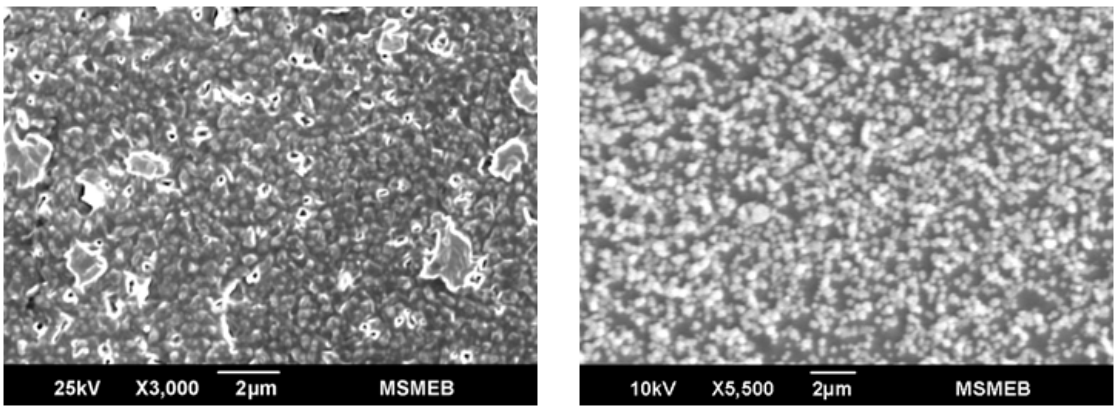

Fig. 1 : SEM images of as-prepared samples (a) TS:P_{EG} nanocomposite, and (b) TS:T_X nanocomposite

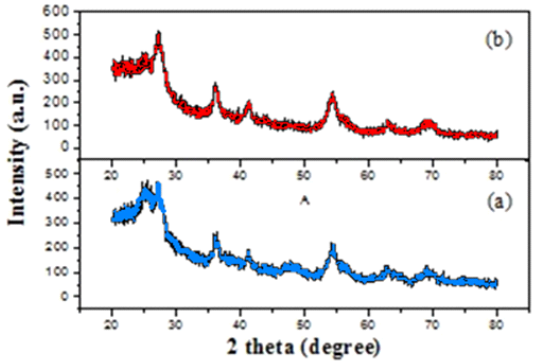

Fig. 2: XRD analysis of (a) TS:P_{EG} nanocomposite, and (b) TS:T_X nanocomposite

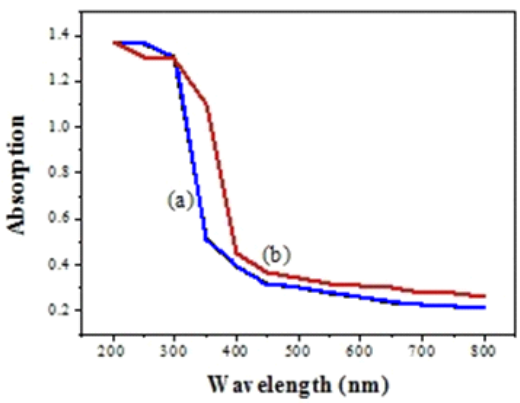

Fig. 3: UV-Visible absorption spectra of (a) TS:P_{EG} nanocomposite, and (b) TS:T_X nanocomposite

There is a wide photoluminescence band in the wavelength range of 410-600 nm. In whole emission spectra the peak is observed at near 434 nm for TS:P_{EG} composite and 434.6 nm for TS:T_X composite. The PL intensity of TS:T_X nanocomposite was decreased compared with TS:P_{EG} nanocomposite. The PL intensity of TS:T_X was reduced and the shape of the PL spectrum obviously split into many side peaks, which shows the formation of resolved manifold lines were located on well-defined lattice sites. The lower PL intensity indicates the decrease in recombination rate, thus shows the higher photocatalytic activity [40]. This results indicated that, the interaction existed between SiO_2 and TiO_2, which cause the formation of the oxygen vacancy, thus to reduced the recombination rate of excited electrons and holes.

FTIR spectroscopic analysis

The FTIR spectra were measured in the spectral range from 400 to 4000 cm^{-1}, and measurements were performed at room temperature. The FTIR spectra of the sol-gel derived nano TS:P_{EG} and TS:T_X samples of TiO_2/SiO_2 composite particles are presented in Fig. 5.

The transmittance in the range from 3612 cm^{-1} to 2862 cm^{-1} may be related to the presence of -OH stretching vibration. The peaks at 1639 cm^{-1} in the spectra are due to the bending vibration of the -OH group which is probably because the re-absorption of water from the atmosphere[41]. In TS:P_{EG}, the IR spectrum shows a weak band peak at about 1512 cm^{-1} corresponding to the bending vibration of -OH groups. In TS:Tx, the IR spectrum shows a

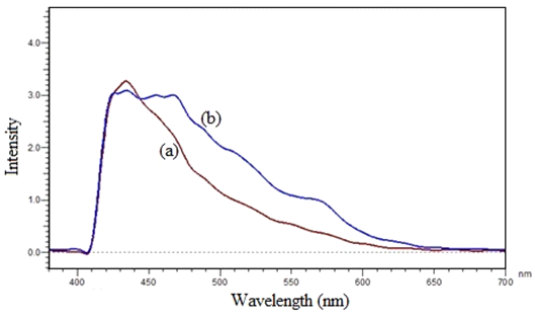

Fig. 4: Photoluminescence emission spectra of (a) TS:P_{EG} nanocomposite, and (b) TS:T_X nanocomposite

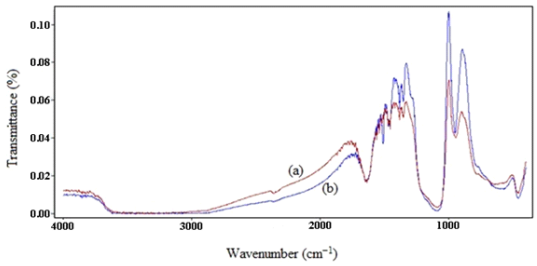

Fig. 5: FTIR spectra of (a) TS:P_{EG} nanocomposite, and (b) TS:T_X nanocomposite

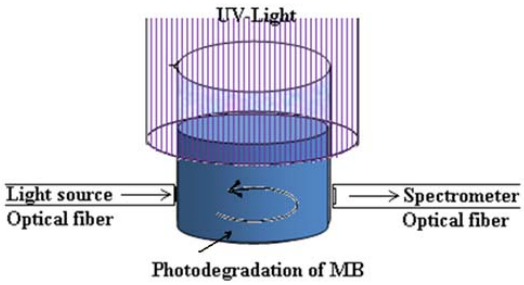

Fig. 6: Schematic photocatalytic degradation Setup

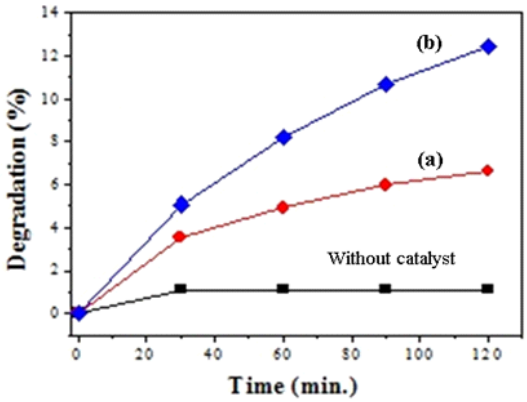

Fig. 7: Photocatalytic degradation study performed under UV light source with Methylene Blue (MB) for the prepared samples (a) TS:P_{EG} nanocomposite, and (b) TS:T_X nanocomposite

strong band peak at about 1512 cm^{-1} corresponding to the bending vibration of -OH groups.

The FTIR spectrum of the samples shows the strong band in the range at 1462 cm^{-1} is associated with the characteristic vibration modes of TiO_2 (Ti-O). The band around at 654 cm^{-1} to 549 cm^{-1} attributes to the Ti-O-Ti stretching vibration of crystalline TiO_2 phase[42]. The band near 1094 cm^{-1} corresponds to the asymmetric stretching vibration of Si-O-Si bond[43]. This confirms that the SiO_2 phase is formed. The band observed at 949 cm^{-1} is associated with Si-O-Ti vibration[28] modes which are due to the overlapping from vibrations of Si-OH and Si-O-Ti bonds. Other peaks appear at 1380 cm^{-1} and 1353 cm^{-1}, which may be attributed to organic solvents these peaks become quite weak and even vanish. These results indicate that TS:P_{EG} and TS:T_X nanoparticles were prepared by a combination of TiO_2 with SiO_2 nanoparticles which corresponds to the metal oxide bonds in both samples.

Photocatalytic activity

The schematic diagram of setup for photocatalytic activity of nanocomposite samples under UV light source is shown in Fig. 6 and The Photocatalytic degradation study results are given in Fig. 7. The adsorption of MB dye without catalyst remains constant and gets saturated after 60 min., indicating that the contribution of self photolysis degradation was negligible. The TS:P_{EG} composite sample exhibited slower rate of the photo degradation. The sample TS:T_X shows the higher photo degradation that must be responsible for the two factors: firstly, surface phenomenon that is being very sensitive to the amount of surface -OH groups which may act as the principal reactive oxidant in the photoreactions[12]. Secondly, the low recombination rate of photo generated electrons and holes which caused the interactions in Ti-Si that improved the separation rate of photo generated electrons and holes, thus leading to the higher photo activity. The TS:T_X absorbs the solute better than the TS:P_{EG} catalyst and exibits remarkable improvement in the rate of photocatalytic degradation of MB. With sample TS:T_X , only after few minute of exposure to UV light, about 50% of the methylene blue was degraded. These results confirms that the TS:T_X nanocomposite crystal exhibit high photocatalytic activity than TS:P_{EG}

CONCLUSION

TiO_2/SiO_2 nanocomposite materials have been successfully synthesized via a simple and cheap non-ionic surfactants assisted sol-gel method. In XRD investigation, the anatase phase of TiO_2 with nano-sized particles was obtained for both the samples. The suppressing effect of SiO_2 on crystal growth of TiO_2 is clearly observed with the addition of Triton X-100 could effectively decrease the crystallite size of TS composite particle. The TS cores were uniformly coated by Triton X-100 exhibited regular morphology and having spherical particles. Analysis of FTIR spectra shows that in nanocomposite structure Si-O-Si, Ti-O and Ti-O-Si bonds have been formed. The absorption spectra of the TS:T_X nanocomposite sample shows better absorbance in visible region compared to TS:P_{EG} nanocomposite particle. In PL optical properties for TS:T_X composite shows lower PL intensity indicates that the decrease in recombination rate, thus higher photocatalytic activity. The TS:T_X nanocomposite shows the higher photocatalytic activity in degradation of MB under UV light irradiation.

ACKNOWLEDGEMENTS

The authors would like to thank UGC-DAE-CSR Indore center, India for XRD characterizations facility.

REFERENCES

1. Oregan, B.; Gratzal, M. *J. Nature* **1991**, *353*, 737-740
2. Kubota, Y.; Niwa, C.; Ohnuma, T.; Ohko, Y.; Talsuma, T.; Mori, T.; Fujishima, A. *J. Photochem. Potoboil*. A **2001**, *141*, 225
3. Tryl, D. A.; Fujishima, A.; Honda, K. *J. Electrochim. Acta* **2000**, *45*, 2363-2376
4. Gonzales, R. J.; Zallen, R.; in: M.F. Thorpe, M.I. Mitkova (Eds.), NATO-ASI. Proceedings, Amorphous Insulators and Semiconductors, Kluwer, Dordrecht, **1997.**
5. Kim, E. J.; Hahn, S. H. *J. Mater. Lett*. **2001**, *49*,

244-249
6. Chen, Y. F.; Lee, C. Y.; Yen, M. Y.; Chiu, H. T. *J. Crystal Growth* **2003**, *247*, 363-370
7. Dhage, S. R.; Choube, V. D.; Samuel, V.; Ravi, V. *J. Mater. Lett.* **2004**, *58*, 2310-2313
8. Burns, A.; Hayes, G.; Li, W.; Hirvonen, J.; Demaree, J. D.; Shah, *S. I. J. Materials Science and Engineering* **2004**, BXXX MSB 9793, 1-6
9. Gugliemi, M.; Colombo, P.; Mancielli, D. *J. Nan-Cryst. Sol.* **1992**, *147*, 641-645
10. Forro, L.; Chauvet, O.; Emin, D.; Zupplioli, L.; Berger, H.; Levy, F. *J. Appl. Phys*. **1994**, *75(1)*, 633-635
11. Liang, Y.; Gan, S.; Chambers, S. A.; Altman, E. I. J. *Physical Review B* **2001**, *63*, 235402-1
12. Hoffmann, M. R.; Martin, S. T.; Choi, W.; Bahnemann, D. W. *J. Chem. Rev*. **1995**, *95*, 69-96
13. Fujishima, A.; Rao, T. N.; Tryk, D. A. J. Photochem. Photobiol., C: *Photochem. Rev.* **2000**, *1(1)*, 1-21
14. Thompson, T. L.; Yates, J. T. *J. Chem. Rev.* **2006**, *106(10)*, 4428-4453
15. Yu, J. G.; Yu, J. C.; Cheng, B.; Zhao, X. J. J. Sol-Gel Sci. and Tech. 2002, 24, 39
16. Rekoske, J. E.; Barteau, M. A. J. Phys. Chem. 1997, B101, 1113-1124
17. Malato, S.; Blanco, J.; Vidal, A.; Alarcon, D.; Maldonado, M. I. J. Caceres, W. Gernjak, *J. Solar Energy* **2003**, *75*, 329-336
18. Pawar, R.P., *Orient J. Chem.* **2013**, *29(3),* 1139-1142.
19. Taghvaei, V.; Yangjeh A. H.; Behboudnia, M. J. *Powder Technol*. **2009**, *195(1)*, 63-67
20. Esmaili, M.; Yangjeh, A. H. *J. Iran. Chem. Soc.* **2010**, *7*, 70-82
21. Jang, H. D.; Kim, S. K.; Kim, S. J. J. *Nanopart. Res*. **2001**, *3*, 141-147
22. Marugan, J.; Lopez, M. J. *Ind. Eng. Chem. Res.* **2006**, *45*, 8900-8908
23. Kumar, A.; Shyla, J. M.; Xavier, F. P. *J. Appl. Nanosci.* **2012**, *2*, 429-436
24. Calleja, G.; Serrano, D. P.; Sanz, R.; Pizarro, P. J. *Microporous and Mesoporous Materials* **2008**, *111*, 429-440
25. Minero, C.; Catozzo, F.; Pelizzetti, E. *J. Langmuir* **1992**, *8*, 481-486
26. Ennaoui, A.; Sankalap, B. R.; Skryshevsky, V.; Lux-Steiner, M. C. J. *Sol Energy Mater. Sol. Cells* **2006**, *90*, 1533-1541
27. Cheng, S.; Tsai, S. J.; Lee, Y. F. J. Catal. Today **1995**, *26*, 87-96
28. Aziz, R. A.; Sopyan, I. *Indian Journal of Chemistry* **2009**, *48A* , 951-957
29. Nilchi, A.; Darzi, S. J.; Garmarodi, S. R. *J. Materials Sciences and Applications* **2011**, *2*, 476-480
30. Kim, S. W.; Kang, M.; Choung, *S. J. J. Ind. Eng. Chem*. **2005**, *11(3)*, 416-424
31. Gao, X.; Wachs, I. E. J. *Catalysis Today* **1999**, *51*, 233-254
32. Hu, S.; Li, F.; Fan, Z. J. *Bull. Korean Chem. Soc*. **2012**, *33(6)*, 1895-1899
33. Mosurkal, R.; Samuelson, L. A.; Smith, K. D.; Westmoreland, P. R.; Parmar, V. S.; Yan, F. J. *Macromolecular Science Part A Pure and Applied Chemistry* **2008**, *45*, 924-46
34. Shao, G. N.; Kim, Y.; Imran, S. M.; Jeon, S. J.; Sarawade, P. B.; Hilonga, A.; Kim, J. K.; Kim, H. T. J. *Microporous and Mesoporous Materials* **2013**, *179*, 111-121
35. Aaritalo, V.; Meretoja, V.; Tirri, T.; Areva, S.; Jamsa, T.; Tuukkanen, J.; Rosling, A.; Narhi, T. *J. Materials Sciences and Applications* **2010**, *1*, 118-126
36. Venckatesh, R.; Balachandaran, K.; Sivaraj, R. *International Nano Letters* **2012,** *2(15)*, 1-5
37. Kimura, I.; Kase, T.; Taguchi, Y.; Tanaka, M. *Materials Research Bulletin*. **2003**, *38(4)*, 585-597.
38. Castro, A. L.; Nunes, M. R. J. *Solid State Sci.* **2008**, *10*, 602-606
39. Yeh, C. L.; Yeh, S. H.; Ma, H. K. *J. Powder Technol*. **2004**, 145, 1-9.
40. Hu, S. Z.; Wang, A. J.; Li, X.; Wang, Y.; Lowe, *H. J. Chem. Asian* **2010**, *5*, 1171-1177.
41. Mohan, J.; "Organic spectroscopy principles and applications", 2nd Eds. Narosha Publishing House Pvt. Ltd, New Delhi, **2009**, 28-95.
42. Lee, J. W.; Kong, S.; Kim, W. S. *J. Mater. Chem. Phys*. **2007**, *106*, 39-44.
43. Yan, X. L.; He, J.; Evans, D. G.; Duan, X.; Zhu, Y. X. *J. Appl. Catal*. **2005**, *B 55*, 243-252.